10216 *Biochemistry* **2010,** *49,* 10216–10227
DOI: 10.1021/bi1010249

BIOCHEMISTRY
including biophysical chemistry & molecular biology
Article

β-Propeller Phytase Hydrolyzes Insoluble Ca^{2+}-Phytate Salts and Completely Abrogates the Ability of Phytate To Chelate Metal Ions[†]

Ok-Hee Kim,[‡,⊥,●] Young-Ok Kim,[●,§] Jae-Hoon Shim,[∥] Yun-Shin Jung,[‡] Woo-Jin Jung,[‡] Won-Chan Choi,[@] Heeseob Lee,[#] Sang-Jun Lee,[§] Kyung-Kil Kim,[§] Joong-Huck Auh,[▽] Hyeonjin Kim,[○] Jung-Wan Kim,[⊥] Tae-Kwang Oh,[@] and Byung-Chul Oh*[,‡]

[‡]*Lee Gil Ya Cancer and Diabetes Institute, Gachon University of Medicine and Science, 7-45 Songdo-dong, Yeonsu-ku, Incheon 406-840, Korea,* [§]*Biotechnology Research Center, National Fisheries Research and Development Institute, 408-1 Sirang-ri, 619-902, Gigang-eup, Gigang-gun, Busan, Korea,* [∥]*Department of Food Science and Nutrition, Hallym University, 39 Hallymdaehak-gil, Chuncheon, Gangwon-do 200-702, Korea,* [⊥]*Department of Biology, University of Incheon, Incheon 406-772, Korea,* [@]*Microbial Genomics and Applications Center, Korea Research Institute of Bioscience and Biotechnology, Yusong, Daejeon 305-333, Korea,* [#]*Department of Food Science and Nutrition, Pusan National University, Busan 609-735, Korea,* [▽]*Department of Food Science and Technology, Chung-Ang University, Anseong 456-756, Korea, and* [○]*Department of Radiology, Seoul National University Hospital, 28 Yongon-dong, Chongno-gu, Seoul 110-744, Korea.* [●]*These authors contributed equally to this work.*

Received June 26, 2010; Revised Manuscript Received September 27, 2010

ABSTRACT: Phytate is an antinutritional factor that influences the bioavailability of essential minerals by forming complexes with them and converting them into insoluble salts. To further our understanding of the chemistry of phytate's binding interactions with biologically important metal cations, we determined the stoichiometry, affinity, and thermodynamics of these interactions by isothermal titration calorimetry. The results suggest that phytate has multiple Ca^{2+}-binding sites and forms insoluble tricalcium- or tetracalcium-phytate salts over a wide pH range (pH 3.0−9.0). We overexpressed the β-propeller phytase from *Hahella chejuensis* (HcBPP) that hydrolyzes insoluble Ca^{2+}-phytate salts. Structure-based sequence alignments indicated that the active site of HcBPP may contain multiple calcium-binding sites that provide a favorable electrostatic environment for the binding of Ca^{2+}-phytate salts. Biochemical and kinetic studies further confirmed that HcBPP preferentially recognizes its substrate and selectively hydrolyzes insoluble Ca^{2+}-phytate salts at three phosphate group sites, yielding the final product, myo-inositol 2,4,6-trisphosphate. More importantly, ITC analysis of this final product with several cations revealed that HcBPP efficiently eliminates the ability of phytate to chelate several divalent cations strongly and thereby provides free minerals and phosphate ions as nutrients for the growth of bacteria. Collectively, our results provide significant new insights into the potential application of HcBPP in enhancing the bioavailability and absorption of divalent cations.

Phytate[1] is a naturally occurring compound and the principal storage form of phosphorus and inositol in many plant tissues, notably bran and seeds (*1*). It is widely found in fruits, vegetables, nuts, organic soils, and marine and freshwater sediments, and its content ranges from 0.17 to 9.15% depending on the food source (*2*). In plant seeds, phytate predominantly occurs in the form of calcium, magnesium, and potassium salts. It also forms a variety of insoluble salts with essential trace element ions, including Co^{2+}, Cu^{2+}, Fe^{3+}, Mn^{2+}, Mo^{2+}, and Zn^{2+} (*3*).

The insolubility of these phytate salts is a major cause of reduced bioavailability of minerals in monogastric animals, such as humans, pigs, poultry, and fish. Monogastric animals secrete insufficient quantities of enzymes into their digestive tracts to fully hydrolyze phytate salts and instead eliminate the mineral-phytate compounds in their feces. The loss of phytate salts contributes to the antinutritional impact of phytate and may result in mineral deficiencies in monogastric animals whose staple diet includes foods with high phytate content (*4*). More specifically, phytate inhibits calcium absorption in animals, leading to diseases such as rickets in dogs, for example (*5*−*7*). Moreover, bread prepared from phytate-rich wheat flour possesses chelating properties that impact the retention of essential minerals by humans (*8*), and phytate degradation improves calcium absorption in humans (*9*). The bioavailability of phosphate and Ca^{2+} in foods can be increased if Ca^{2+}-phytate salts are degraded, and thus, the removal of phytate from food may be of considerable nutritional significance.

Phytases make up a group of inositol phosphate phosphatases that are responsible for the hydrolysis of phytate. They exist widely in a variety of microorganisms and plants. On the basis of structural differences and biochemical characteristics, phytases

[†]This study was supported by the 21C Frontier Microbial Genomics and Applications Center Program (11-2008-18-001-00, B.-C.O.), Ministry of Education, Science and Technology, Republic of Korea, and in part by a research grant (Y.-O.K.) from the National Fisheries Research and Development Institute, Republic of Korea.

*To whom correspondence should be addressed. E-mail: bcoh@gachon.ac.kr or byungcoh@hotmail.com. Phone: 82-32-899-6074. Fax: 82-32-899-6075.

[1]Abbreviations: BPP, β-propeller phytase; BaBPP, β-propeller phytase from *Bacillus amyloliquefaciencs*; HcBPP, β-propeller phytase from *Hahella chejuensis*; HAPs, histidine acid phytases; InsPs, myo-inositol phosphates; IPTG, isopropyl β-D-thiogalactopyranoside; ITC, isothermal titration calorimetry; HPIC, high-performance ion chromatography; phytate (InsP6), myo-inositol 1,2,3,4,5,6-hexakisphosphate; SDS−PAGE, sodium dodecyl sulfate−polyacrylamide gel electrophoresis.

 Published on Web 10/21/2010

are classified into three major subclasses: the histidine acid phosphatases (HAPs), the β-propeller phytases (BPPs), and the purple acid phosphatases (PAPs) (*10*, *11*). Of these, the BPPs, which have been extensively characterized in *Bacillus* spp., have high thermal stability, an optimal pH of approximately 7.0−8.0, and strict substrate specificity for phytate (*12*, *13*). The crystal structure of BPP includes multiple calcium-binding clefts and two phosphate group binding sites with six-blade β-propeller structures (*14*, *15*). We previously characterized the kinetic mechanism of BPP, as well as the roles of essential catalytic amino acid residues and substrate specificity determinants (*16*, *17*).

Bioinformatic studies on microbial genomes from the NCBI database have indicated that BPPs are widespread in prokaryotes but do not exist in higher eukaryotes with the exception of fungal species, in which BPP enzymatic activity has not yet been determined (*18*, *19*). Although enzymatic properties of BPPs from *Bacillus* spp. (*11*), *Shewanella oneidensis* MR-1 (*18*), and *Pedobacter nyacknesis* MJ11CGMCC 2503 (*20*) have been characterized, little is known about the kinetic properties of other BPPs. Furthermore, the precise mechanisms by which BPP hydrolyzes insoluble mineral-phytate salts have not been investigated in aquatic systems.

We examined BPP from the aquatic bacterium *Hahella chejuensis* (HcBPP) to gain insight into the biochemical and kinetic properties of BPPs from aquatic microorganisms. We also analyzed the thermodynamics of the interactions of phytate with important minerals to improve our understanding of the physicochemical properties of mineral-phytate complexes. Defining the substrate specificities of BPPs from aquatic bacteria will be important in explaining how insoluble Ca^{2+}-phytate salts are processed in biological systems. We have discovered a novel kinetic mechanism in HcBPP that efficiently hydrolyzes insoluble Ca^{2+}-phytate salts.

Our results indicate that HcBPP efficiently abrogates the ability of phytate to chelate Ca^{2+} and other divalent cations by hydrolyzing every second phosphate in phytate, thereby generating Ins(2,4,6)P_3. The total elimination of phytate's capacity to chelate specific minerals is a highly desirable property of HcBPP that may be useful in biotechnology and nutritional applications.

EXPERIMENTAL PROCEDURES

Materials. Plasmid DNA was prepared using Miniprep kits (Qiagen, Inc., Valencia, CA). Restriction fragments and PCR products were purified from agarose gels using the QIAquick gel extraction kit (Qiagen, Inc.). All other reagents were obtained from Sigma-Aldrich (St. Louis, MO) unless otherwise indicated.

Cloning of the Phytase Gene from H. chejuensis and Overexpression of Phytase in Escherichia coli. The amino acid sequence of the β-propeller phytase protein from *Bacillus amyloliquefaciens* DS11 was used to screen other BPPs listed in the SMART database (http://smart.embl-heidelberg.de/). These database searches enabled us to identify the amino acid sequences of 66 BPPs that have a six-blade propeller folding architecture. Among these sequences, we selected one from the Oceanospirillales bacterium *H. chejuensis* KCTC 2396 for biochemical characterization. The *H. chejuensis* gene encoding β-propeller phytase (amino acid residues 21−451) was subcloned into the pACYC duet (Novagen) vector to generate a protein with a C-terminal six-His tag or was subcloned into the pGFPuv (Clontech) vector to generate a fusion protein with a C-terminal GFP tag. The following oligonucleotides were used as primers in polymerase chain reactions (PCRs): PN21_HC_Phy (NcoI), 5′ AAACCATGGCTCCTCCCGAAGTTGTCGCT 3′; PC451_HC_Phy (XhoI), 5′ AAACTCGAGATGGGGGAACCGGTGCTTCC 3′; PN_21_HC_Phy (HindIII), 5′ CCCAAGCTTGGCTCCTCCCGAAGTTGTCGC 3′; and PC_450_HC_Phy (XbaI), 5′ AAATCTAGAGTATGGGGGAACCGGTGCTTCC 3′. Site-specific mutagenesis was performed using a QuickChange site-directed mutagenesis kit (Stratagene). The following oligonucleotides were used as mutagenic primers: PN_E245A, 5′ CCGCAAGTGGCAGGCATGGTGATCGATGAG 3′; PC_E245A, 5′ CACCATGCCTGCCACTTGCGGGTCCTGGCC 3′; PN_322A, 5′ GCGGATGTCGCAGGGCTGACCATCTATTAC 3′; and PC_322A, 5′ GGTCAGCCCTGCGACATCCGCTTTCAGATG 3′. Following PCR, the amplified DNA fragments were ligated with T4 DNA ligase. The ligation mixture was used to transform competent *E. coli* XL1 Blue cells. Colonies were isolated, and plasmid DNA was extracted using QIAGEN Miniprep kits. A plasmid harboring the β-propeller phytase gene from *H. chejuensis* was introduced into competent *E. coli* BL21(DE3) cells. Initially, the cells were grown in 50 mL of LB-chloramphenicol (20 μg/mL) for 8 h at 37 °C before being inoculated into 2 L of LB-chloramphenicol (20 μg/mL) and then transferred immediately to a shaking incubator at 30 °C. When the cultures reached an absorbance at 600 nm of 0.6−1.0, isopropyl β-D-thiogalactopyranoside (IPTG) was added to a final concentration of 1 mM to induce the expression of *H. chejuensis* β-propeller phytase. After 4−5 h, the cells were harvested and lysed by sonication in equilibrium buffer [150 mM NaCl and 50 mM Tris-HCl (pH 7.6)]. The enzyme was purified using Ni NTA (QIAGEN) and gel filtration chromatography (using Superdex-200). The purity of the β-propeller phytase obtained was determined by SDS−PAGE. All of the data presented in this study were obtained using this purified phytase.

Phytase Assay. The enzyme's phytase activity was assessed by measuring the production of inorganic orthophosphate (P_i) using the method described previously (*11*, *16*). In brief, experiments were conducted in 100 mM Tris-HCl (pH 7.0) using various concentrations of Na-phytate (0.01−5.0 mM) and Ca^{2+} (0−12 mM). To measure Ca^{2+} ion activation, a Chelex 100 resin (Na form, 200−400 mesh, Bio-Rad) was added to each solution to remove contaminating metal ions, including Ca^{2+}, and the solutions were stirred for 60 min. After filtration, the pH of the solution was measured and adjusted, if necessary, using 0.1 N HCl or 0.1 N NaOH. Enzymatic reactions were initiated via addition of 50 μL of enzyme that had been preincubated with increasing concentrations of Ca^{2+}, followed by 450 μL of 1.1 mM Na-phytate that had been preincubated with 100 mM Tris-HCl solutions of the appropriate pH containing different concentrations of Ca^{2+}. The reactions were arrested via addition of 500 μL of a coloring reagent solution containing 2.5% ammonium heptamolybdate, 0.175% ammonia, 0.1425% ammonium vanadate, and 22.75% nitric acid. The absorbances of the resulting mixtures were measured at 415 nm.

Thermodynamics of Divalent Metal Ion Binding to Phytate or Ins(2,4,6)P_3. To measure the binding isotherms for the binding of divalent metal ions, including Ca^{2+}, Co^{2+}, Fe^{3+}, Mg^{2+}, Mn^{2+}, Sr^{2+}, and Zn^{2+}, to phytate or Ins(2,4,6)P_3, isothermal titration calorimetry (ITC) experiments were performed using a MicroCal 200 isothermal titration microcalorimeter (MicroCal, Northampton, MA). Data collection, analysis, and plotting were performed using Windows-based Origin version 7.0 (MicroCal). The titrating microcalorimeter contained

sample and reference cells held in an adiabatic enclosure. The reference cell was filled with distilled water. Typical titrations involved injection of 1.5 μL of each metal ion at concentrations of 5−15 mM (using a computer-controlled injector) into the sample cell [filled with 0.5 mM phytate or 0.5 mM Ins(2,4,6)P_3 solutions at different pHs]. Samples were injected at 2 min intervals to ensure that the titration curves had returned to baseline before the next injection. The syringe stir rate was set to 1000 rpm. The absorption or release of heat during each injection was measured using the calorimeter. Titration isotherms for the binding interactions comprised the differential heat flows for the different injections. These values were integrated to determine the enthalpy change associated with each injection. The heat changes caused by the injection of each metal ion into distilled water were negligible. The dilution data were subtracted from the sample data, and then bad data points were removed. The data fitting was performed using Origin version 7.0, and the fitting process was iterated until the best fit was obtained, as determined by the χ^2 minimization method (*21*, *22*). Fitting the binding isotherms in this way provided data about the binding constant (K_a), the change in enthalpy (ΔH), and the stoichiometry of binding (n). The binding Gibbs free energy (ΔG) was calculated from the enthalpy change (ΔH) and binding constant (K_a) using the equation $\Delta G = RT \ln K_a = \Delta H \times T\Delta S$, where R is the gas constant and T is the absolute temperature in kelvin (*23*). The stoichiometries (n) of the different interactions were determined from the One Set of Sites and Two Sets of Sites models.

Calculation of [Ca^{2+}], [*Phytate*], [Ca^{2+}-*Phytate*], *and* [$(Ca^{2+})_3$-*Phytate*] *as a Function of* [Ca^{2+}] *or as a Function of* [*Phytate*]. The initial velocity in a solution containing 0.003 M total Ca^{2+} and various concentrations of total phytate from 0.0005 to 0.004 M or vice versa was examined by considering the following system involving Ca^{2+}-phytate and $(Ca^{2+})_3$-phytate:

$$Ca^{2+} + \text{phytate} \underset{K_{d1}}{\leftrightarrow} Ca^{2+}\text{-phytate} + 2Ca^{2+} \underset{K_{d2}}{\leftrightarrow} (Ca^{2+})_3\text{-phytate}$$

where $K_{d1} = [Ca^{2+}][\text{phytate}]/[Ca^{2+}\text{-phytate}] = 0.00000662$ M and $K_{d2} = [Ca^{2+}\text{-phytate}][Ca^{2+}]^2/[(Ca^{2+})_3\text{-phytate}] = 0.00005025$ M, from the ITC analysis of Ca^{2+} binding to phytate at pH 5.0. In this work, K_{d1} is the dissociation constant for Ca^{2+}-phytate, K_{d2} is the dissociation constant for $(Ca^{2+})_3$-phytate, x is the Ca^{2+} concentration, y is the phytate concentration, z is the Ca^{2+}-phytate concentration, and w is the $(Ca^{2+})_3$-phytate concentration, based on the measured dissociation constants from the ITC analysis for Ca^{2+} binding to phytate at pH 5.0.

Suppose that we wish to measure the initial velocity in a solution containing 0.003 M total Ca^{2+} and some concentration of total phytate (e.g., 0.0005 M). In the solution containing 0.0005 M total phytate, where $x + z + 3w = 0.003$ and $y + z + w = 0.0005$, we have the following equations:

$$x + z + 3w = 0.0005 \quad (1)$$

$$y + z + w = 0.003 \quad (2)$$

$$xy = 0.00000662z \quad (3)$$

$$z \times x^2 = 0.00005025w \quad (4)$$

We used MATLAB 2008a (MathWorks) to solve these equations for x, y, z, and w. The final output was as follows: $x = 0.00332112$, $y = 8.1593 \times 10^{-7}$, $z = 0.000409335$, and $w = 8.98487 \times 10^{-5}$. The solution with the larger value can be ignored because [Ca^{2+}-phytate] and [$(Ca^{2+})_3$-phytate] cannot exceed 0.0005 M (phytate is limiting).

HPIC Analysis of Reaction Products and Purification of Ins(2,4,6)P_3. The reaction products of the hydrolysis of Ca^{2+}-phytate salts by HcBPP were analyzed using a high-performance ion chromatography (HPIC) system (ICS-3000, Dionex, Sunnyvale, CA), according to the method of Talamond et al. (*24*) with slight modifications. An inositol phosphate analytical column (Omnipac PAX-100, Dionex) and a conductivity detector (Dionex) were used in conjunction with an anion suppressor. Filtered samples (20 μL) were eluted in a 1.5% isopropyl alcohol solution, using a linear NaOH solution gradient (from 70 to 150 mM, 25 min). The separated inositol phosphates were then detected using a conductivity detector (Dionex). In a separate experiment, the final product, Ins(2,4,6)P_3, was purified by recycling HPLC using a chromatography system (LC-918, JAI, Tokyo, Japan) attached to a polymeric gel filtration column (JAIGEL W-251, 30 cm × 2 cm, JAI) and a UV detector (254 nm, JAI). Distilled water, at a flow rate of 3.5 mL/min, was used as the mobile phase. Purified Ins(2,4,6)P_3 was concentrated using a SpeedVac (Eppendorf), and inorganic phosphate was quantified after being boiled in a 10% H_2SO_4 solution.

RESULTS

ITC Analysis of a Metal Cation Binding to Phytate. Phytate binds to divalent and trivalent cations, including Fe^{3+}, Co^{2+}, Cu^{2+}, Mg^{2+}, Sr^{2+}, and Zn^{2+}, and forms insoluble metal-phytate salts (*1*, *2*, *25*). However, questions relating to phytate's relative binding affinity for these cations remain to be answered. To this end, we quantified the binding affinities of divalent and trivalent cations for phytate (in 10 mM sodium acetate at pH 5.0 and 37 °C) and the associated thermodynamic properties by ITC. We performed the ITC experiments at pH 5.0 because of the strong tendency of Fe^{3+} and Zn^{2+} to form precipitates with phytate at a neutral pH.

The ITC data for the binding of divalent and trivalent cations to phytate are shown in Figure 1. The data relating to the heat changes that accompany the binding of metal ions to phytate are shown in the top panels of each figure. The binding isotherms, which correspond to plots of integrated heats as a function of the molar ratio of metal ion to phytate, are shown in the bottom panels of each figure. For Fe^{3+} and Ca^{2+}, a reasonable fit can be achieved with a two-site set model in which ions bind one set of sites with high affinity and another set with low affinity (Figure 1A). On the other hand, the isotherms for the other divalent cations (Co^{2+}, Cu^{2+}, Mg^{2+}, Sr^{2+}, and Zn^{2+}) fit a one-site model, in which the divalent cations bind to one or two independent sites in the phytate molecule. Solid lines indicate the best-fit curves for the two types of models. The thermodynamic parameters corresponding to the binding of divalent and trivalent cations to phytate are listed in Table 1.

The ITC data indicated that phytate binds divalent and trivalent cations with a relatively high affinity (K_d = 0.77−151.06 μM), even at acidic pH (pH 5.0). Among the tested cations, Fe^{3+} bound with the strongest affinity. On the basis of the data listed in Table 1, the ITC data show that metal cations bound to phytate with the following order of relative affinities: $Fe^{3+} > Ca^{2+} > Mn^{2+} > Cu^{2+} > Co^{2+} > Sr^{2+} > Mg^{2+} > Zn^{2+}$. Interestingly, the stoichiometry of the interaction of Ca^{2+} with phytate was quantified as being approximately 3:1, indicating that phytate

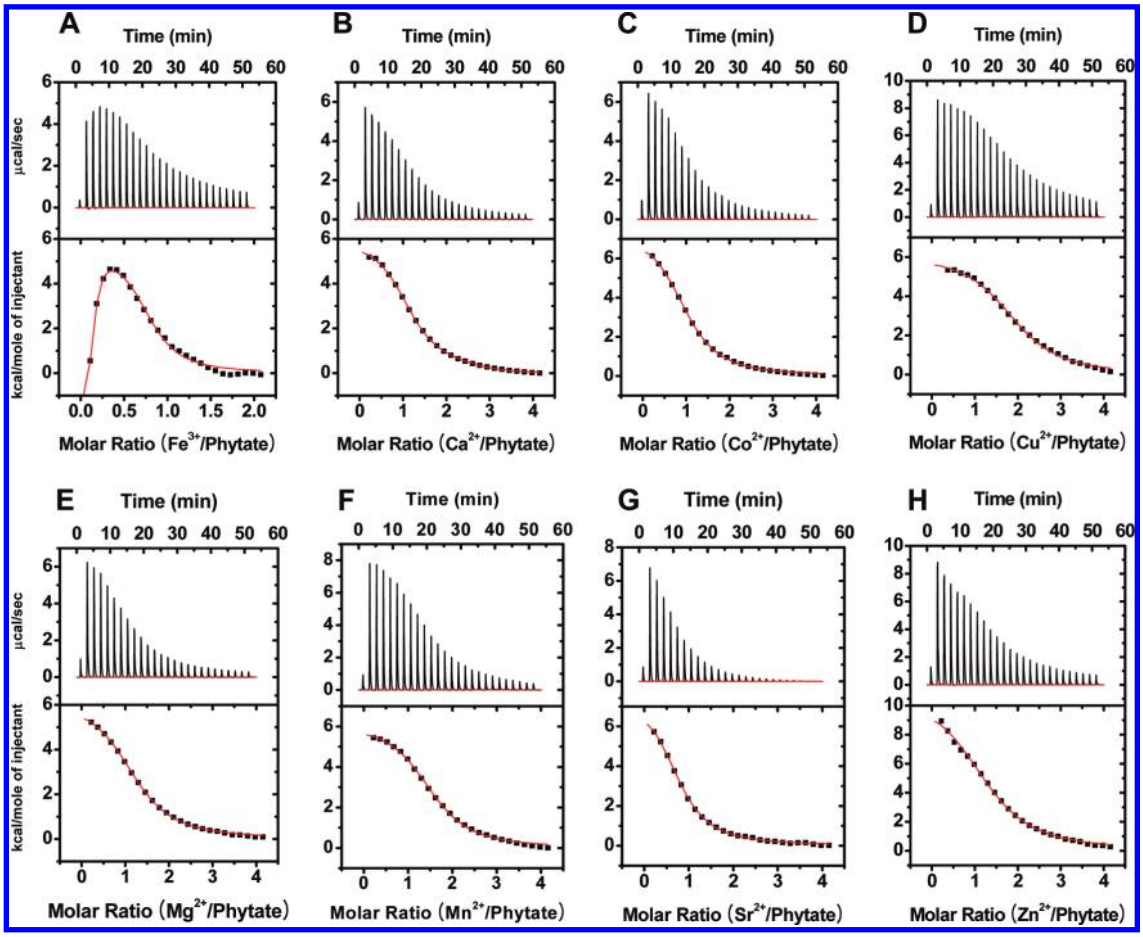

FIGURE 1: ITC analysis of various metal ions binding to phytate. ITC was used to study the kinetics of the binding of Fe^{3+}, Ca^{2+}, Cu^{2+}, Co^{2+}, Mg^{2+}, Mn^{2+}, Sr^{2+}, and Zn^{2+} to phytate at pH 5.0 and 37 °C. For each titration, raw data are shown in the top panel and integrated heat data (corrected for dilution) are shown in the bottom panel. Further details, including calculated association constants and the enthalpy and entropy of the different associations, are presented separately in Table 1.

Table 1: Thermodynamic Parameters of Metal Cations Binding to Phytate Determined by ITC[a]

	Fe^{2+}	Ca^{2+}	Co^{2+}	Cu^{2+}	Mg^{2+}	Mn^{2+}	Sr^{2+}	Zn^{2+}
K_{d1} ($\times 10^{-6}$ M)	0.77	3.53	91.74	86.21	102.77	70.92	101.42	151.06
n_1	0.12	1.05	1.01	1.96	1.25	1.59	0.79	1.34
ΔG_1 (kcal/mol)	−8.69	−7.82	−5.72	−5.77	−5.67	−5.88	−5.66	−15.33
ΔH_1 (kcal/mol)	−2.27	6.01	7.54	6.10	6.30	5.93	7.80	1.10
ΔS_1 (cal mol^{-1} °C^{-1})	20.70	44.60	42.80	38.30	38.60	38.10	43.40	53.00
K_{d2} ($\times 10^{-6}$ M)	28.90	48.78						
n_2	0.65	1.76						
ΔG_2 (kcal/mol)	−6.43	−6.10						
ΔH_2 (kcal/mol)	5.78	0.31						
ΔS_2 (cal mol^{-1} °C^{-1})	39.40	20.70						

[a]The experiments were performed at 310 K with a 0.5 mM phytate solution at pH 5.0. The *n* value represents the number of bound metal ions per phytate molecule. The thermodynamic parameters are given for the association reaction.

forms tricalcium-phytate salts at pH 5.0. These ITC data suggest that the formation of such mineral-phytate salts may affect the bioavailability and absorption of important minerals (*26*−*28*) and may represent an important cause of calcium (*29*−*31*) and iron deficiency in the Western world (*3*, *32*−*36*) and mineral deficiency in vegetarians (*37*−*39*).

ITC Analysis of Ca^{2+} Binding to Phytate. Phytate forms stable complexes with several trivalent and divalent cations such as Fe^{3+}, Ca^{2+}, Co^{2+}, Cu^{2+}, Mg^{2+}, Mn^{2+}, Sr^{2+}, and Zn^{2+} because of the strong negative charges on its six phosphate groups. Among the complexes formed, Ca^{2+}-phytate is typically one of the most prevalent, because Ca^{2+} is the most abundant divalent cation under physiological conditions. Therefore, we analyzed the binding of Ca^{2+} to phytate over a wide pH range (pH 2.0−9.0) by ITC to investigate the thermodynamic properties of this interaction under conditions that model those found in the gastrointestinal (GI) tract.

Representative ITC data relating to the binding of Ca^{2+} to phytate at pH 3.0, 6.0, and 9.0 are shown in Figure 2, while further details, including calculated association constants and the enthalpy and entropy of associations at different pHs, are listed in Table 2. ITC analysis indicated that the Ca^{2+}-phytate binding reaction has the following characteristics. Phytate contains three or four Ca^{2+}-binding sites; Ca^{2+} binds as a function of pH, and

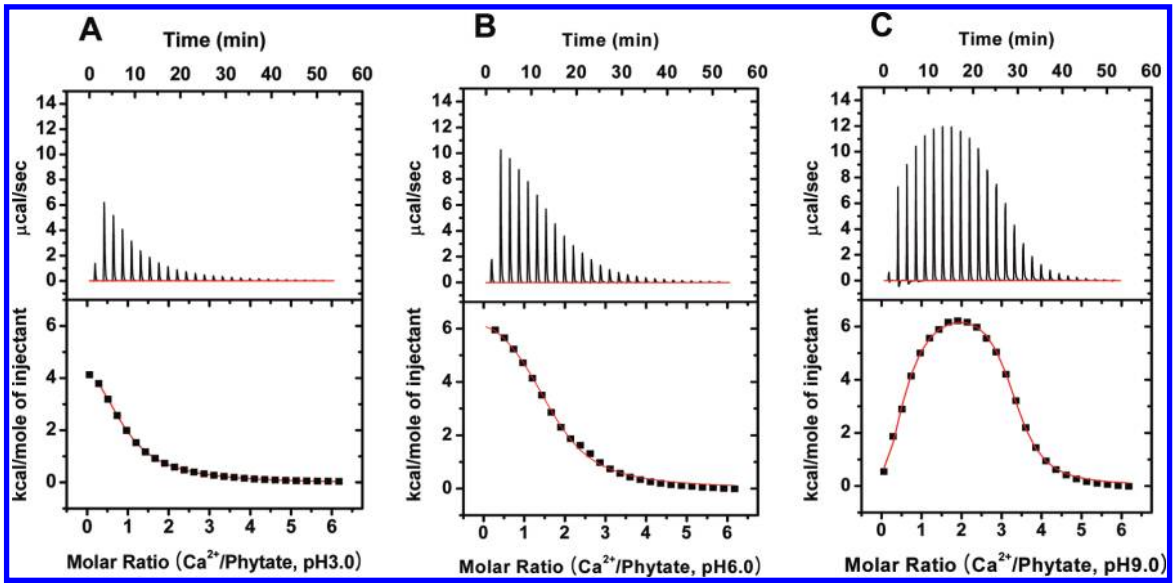

FIGURE 2: ITC analysis of calcium ions binding to phytate. Three representative isotherms are shown illustrating binding as a function of pH at 37 °C. Panels A−C show the results of calorimetric titration of 1.5 μL of 15 mM Ca^{2+} into 0.5 mM phytate solutions at pH 3.0, 6.0, and 9.0, respectively. For each titration, raw data are shown in the top panel and integrated heat data (corrected for dilution) are shown in the bottom panel. Further details, including calculated association constants and the enthalpy and entropy of the different associations, are presented separately in Table 2.

Table 2: Thermodynamic Parameters of Ca^{2+} Binding to Phytate over a pH Range of 2.0−9.0 Determined by ITC[a]

	pH 2	pH 3	pH 4	pH 5	pH 6	pH 7	pH 8	pH 9
K_{d1} ($\times 10^{-6}$ M)	328.95	19.16	1.92	6.62	6.10	3.94	8.77	2.71
n_1	0.80	0.72	0.89	1.12	1.27	0.54	0.10	0.45
ΔG_1 (kcal/mol)	−4.95	−6.68	−8.09	−7.34	−7.40	−7.65	−7.16	−7.89
ΔH_1 (kcal/mol)	7.58	5.90	6.05	6.14	7.05	6.92	−3.47	−4.44
ΔS_1 (cal mol^{-1} °C^{-1})	40.40	40.60	45.60	43.50	46.60	47.00	11.90	11.10
K_{d2} ($\times 10^{-6}$ M)		195.31	23.53	50.25	60.61	94.34	44.84	23.31
n_2		2.73	3.11	1.50	2.01	1.84	2.52	2.77
ΔG_2 (kcal/mol)		−5.25	−6.56	−6.11	−5.99	−5.72	−6.17	−6.56
ΔH_2 (kcal/mol)		0.21	0.04	0.86	0.80	5.72	6.76	7.26
ΔS_2 (cal mol^{-1} °C^{-1})		17.60	21.30	22.50	21.90	36.90	41.70	44.60

[a]The experiments were performed at 310 K with a 0.5 mM phytate solution at each pH. The *n* value represents the number of bound metal ions per phytate molecule. The thermodynamic parameters are given for the association reaction.

one set of sites binds Ca^{2+} with high affinity and a second set with low affinity. The results indicate that Ca^{2+} binds to phytate with high affinity (K_d = 1.92−8.77 μM) but also to low-affinity (K_d = 23.31−94.34 μM) sites in a pH range of 4.0−9.0. Maximal Ca^{2+} binding was observed at pH 4.0 (at this pH, tetracalcium-phytate salts appeared to form). The number of bound Ca^{2+} ions per phytate molecule remained relatively constant in the pH range of 3.0−9.0, but the binding affinity decreased dramatically at pH < 3.0. Ca^{2+} did bind to phytate at pH 2.0; however, the number of bound Ca^{2+} ions per phytate molecule appeared to be only 0.80, and binding affinity was low (K_d = 328.95 μM). These data suggest that Ca^{2+} and phytate combine to form tricalcium- and/or tetracalcium-phytate salts at pH 3.0−9.0 and a monocalcium-phytate salt at pH 2.0. The calculated stoichiometry was slightly lower than that determined previously by equilibrium dialysis with excess Ca^{2+}, which showed that on average, five molecules of Ca^{2+} bound to each phytate molecule (*40*, *41*).

Overexpression of the H. chejuensis Gene That Encodes β-Propeller Phytase. HcBPP was successfully overexpressed in recombinant *E. coli* strain BL21(DE3). The molecular mass of the purified enzyme (measured by SDS−PAGE) was ~68 kDa (Figure S2 of the Supporting Information), somewhat different from the deduced molecular mass (51 kDa), presumably because of the high content of negatively charged amino acids (approximately 21%). Analysis of the HcBPP gene showed that it was strongly homologous to BPPs of various sources. The predicted amino acid sequence of HcBPP was 41% identical to that of *S. oneidensis* BPP (*42*), 63% identical to that of *P. nyackensis* BPP (*20*), and 65−66% identical to that of BPPs from *Bacillus* spp. (*12*, *13*). However, it shared no significant sequence homology with any histidine acid phytase.

Moreover, structure-based sequence alignment of HcBPP with BPP from *B. amyloliquefaciens* (BaBPP) (*14*) revealed some interesting features (Figure S1 of the Supporting Information). HcBPP contains extra-long loops separating its β-sheets. Each loop is 3−26 amino acid residues longer than the equivalent loop in BPPs from *Bacillus* spp. and is characterized by a high percentage of negatively charged residues. The negatively charged side chains of these loop regions may provide a favorable electrostatic environment for the binding of Ca^{2+}-rich phytate salts (e.g., tricalcium- or tetracalcium-phytate salts). The structure-based substitution of Glu245 or Glu322 with alanine in the Ca^{2+}-binding sites at the active sites resulted in the complete loss of enzymatic activity. These results indicated that the Ca^{2+}-binding

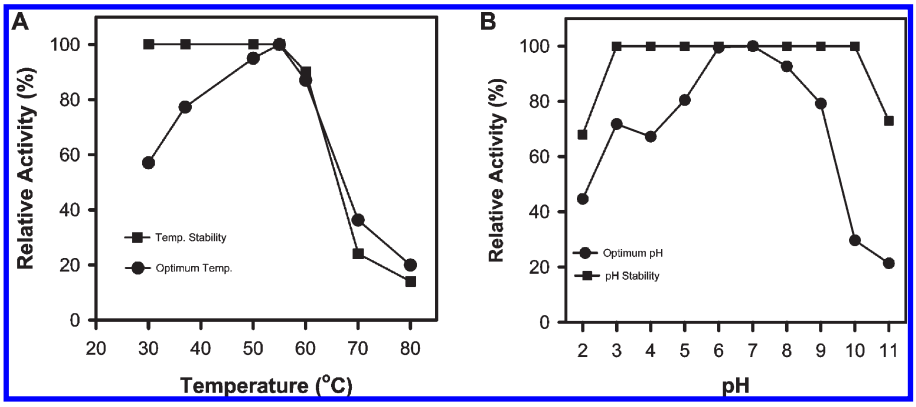

FIGURE 3: Effects of temperature and pH on the hydrolysis of Ca^{2+}-phytate. (A) The enzyme HcBPP was preincubated at various temperatures for 30 min in the presence of 10 mM Ca^{2+} (■), and the residual activity at 55 °C in 50 mM Tris-HCl (pH 7.0) was measured. The enzyme activity in 50 mM Tris-HCl (pH 7.0) was assayed at various temperatures using a substrate prepared by mixing 1 mM phytate and 3 mM Ca^{2+}. (B) Phytase activity at 55 °C was measured in solutions at varying pH values (●). In the pH stability test (■), HcBPP was preincubated with buffers at various pH values for 24 h at 4 °C and the residual activity at 55 °C in 50 mM Tris-HCl (pH 7.0) was measured. The optimal temperature for the hydrolysis of Ca^{2+}-phytate by HcBPP was approximately 55 °C, and the optimal pH was 7.0.

sites of β-propeller phytases in the active site cleft are highly conserved among the β-propeller phytases (Figure S1 of the Supporting Information).

Enzymatic Properties of HcBPP. The enzymatic activity of HcBPP was assayed using Ca^{2+}-phytate salts, prepared by mixing 1 mM Na-phytate and 3 mM Ca^{2+} in 50 mM Tris-HCl at pH 7.0 and various temperatures. The optimal temperature for the hydrolysis of Ca^{2+}-phytate by HcBPP was approximately 55 °C. The enzyme was stable at temperatures up to 55 °C in the presence of 5 mM Ca^{2+}, but the stability decreased dramatically above 65 °C. Nonetheless, the enzyme retained more than 30% of its activity following incubation at 70 °C for 30 min (Figure 3A). When viewed alongside structural data relating to BaBPP, these results indicate that binding Ca^{2+} increases the thermal stability of HcBPP, although it is much lower than that of BaBPP. Structural differences may explain the differential thermal stabilities of these BPPs. As shown in Figure 3B, at 55 °C, maximal HcBPP activity was observed at pH 7.0. Interestingly, the pH profile of the enzyme contained peaks at pH 3.0 and 7.0, with the activity at pH 3.0 approximately 70% of the peak activity (which occurred at pH 7.0). HcBPP retained more than 65% of the maximal activity in the pH range of 3.0−9.0. In addition, it was stable over the broad pH range of 3.0−10.0. Its unique dual-peak pH profile may be significant for the potential biotechnology applications of HcBPP, particularly for reducing the antinutritional effects of foods with high Ca^{2+}-phytate content in the gastrointestinal tracts of monogastric animals. In addition, the pH profile of HcBPP, together with the ITC data, reveals important biophysical properties of phytate and shows that it exists as Ca^{2+}-phytate salts in acidic pH ranges similar to those found in the stomach.

Effect of Ca^{2+} on β-Propeller Phytase Activity. Our kinetic data suggest that BPP requires Ca^{2+} for its catalytic activity, not only as an essential activator but also as a component of its substrate, Ca^{2+}-phytate salts. Several experiments were performed to determine how Ca^{2+} ions affect the activity of HcBPP. Increasing the concentration of Ca^{2+} enhanced the phytase activity in a saturating manner to yield the Hill coefficient ($h = 4.23 \pm 0.16$), indicating that enzyme activation involved a minimum of five Ca^{2+}-binding sites and that phytase activation was mediated by cooperative interactions between Ca^{2+} and the enzyme or substrate (Figure 4A). Furthermore, these results suggest that the enzyme requires a high Ca^{2+} concentration to hydrolyze phytate. In this regard, HcBPP differs markedly from BaBPP, which required a relatively lower Ca^{2+} concentration to be active catalytically (Figure 4D) (*16*, *18*, *43*, *44*). The results confirm that HcBPP requires more Ca^{2+} ions than BaBPP for catalytic activity (Figure 4A,D).

To improve our understanding of the kinetic mechanism behind the hydrolysis of phytate by HcBPP, and the specific role of high Ca^{2+} concentrations, enzymatic activities were measured using a single fixed concentration of phytate (1 mM) and Ca^{2+} concentrations ranging from 0 to 6 mM. The reaction rate peaked at a Ca^{2+} concentration of 3 mM. However, the enzymatic activity began to decline when the Ca^{2+} concentration increased above 4 mM (Figure 4B). Analogously, the phytase activity was measured using a fixed concentration of Ca^{2+} (1 or 2 mM) and phytate concentrations ranging from 0 to 4.0 mM. As expected, the reaction rate increased with phytate concentration. However, increasing the overall phytate concentration beyond an equivalent Ca^{2+} concentration resulted in a significant decrease in the reaction rate (Figure 4C), indicating that the concentration of Ca^{2+}-free phytate (i.e., not complexed with Ca^{2+}) had increased (Figures 4C and 5C,D) and that excess amounts of phytate (Ca^{2+}-free phytate) can be a competitive inhibitor of the enzyme, as the β-propeller phytase can bind only the Ca^{2+}-phytate salt as a substrate at the active site (Figure 4H,I). The results confirmed that the activity of HcBPP (Figure 4C) is more strongly inhibited by Ca^{2+}-free phytate than that of BaBPP (Figure 4F). The results presented in this and previous sections suggest that the rate of phytate hydrolysis depends on the relative concentrations of Ca^{2+} and phytate when the molar ratio of Ca^{2+} to phytate reaches approximately 3−4. Under these conditions, phytate tends to exist as insoluble Ca^{2+}-phytate salts (Figure 4B). Thus, it appears that HcBPP requires high Ca^{2+} concentrations to be active enzymatically and that it efficiently hydrolyzes insoluble Ca^{2+}-phytate salts. From a physicochemical perspective, it seems reasonable to assume that Ca^{2+}-phytate salts sinking from the euphotic zone at the surface of the ocean might precipitate at greater depths as insoluble Ca^{2+}-phytate salts (*18*, *19*). In this regard, our results suggest that BPPs in marine bacteria are able to hydrolyze insoluble Ca^{2+}-phytate salts, thereby releasing free inorganic phosphate, which may serve as a nutrient to support their survival in the deep ocean.

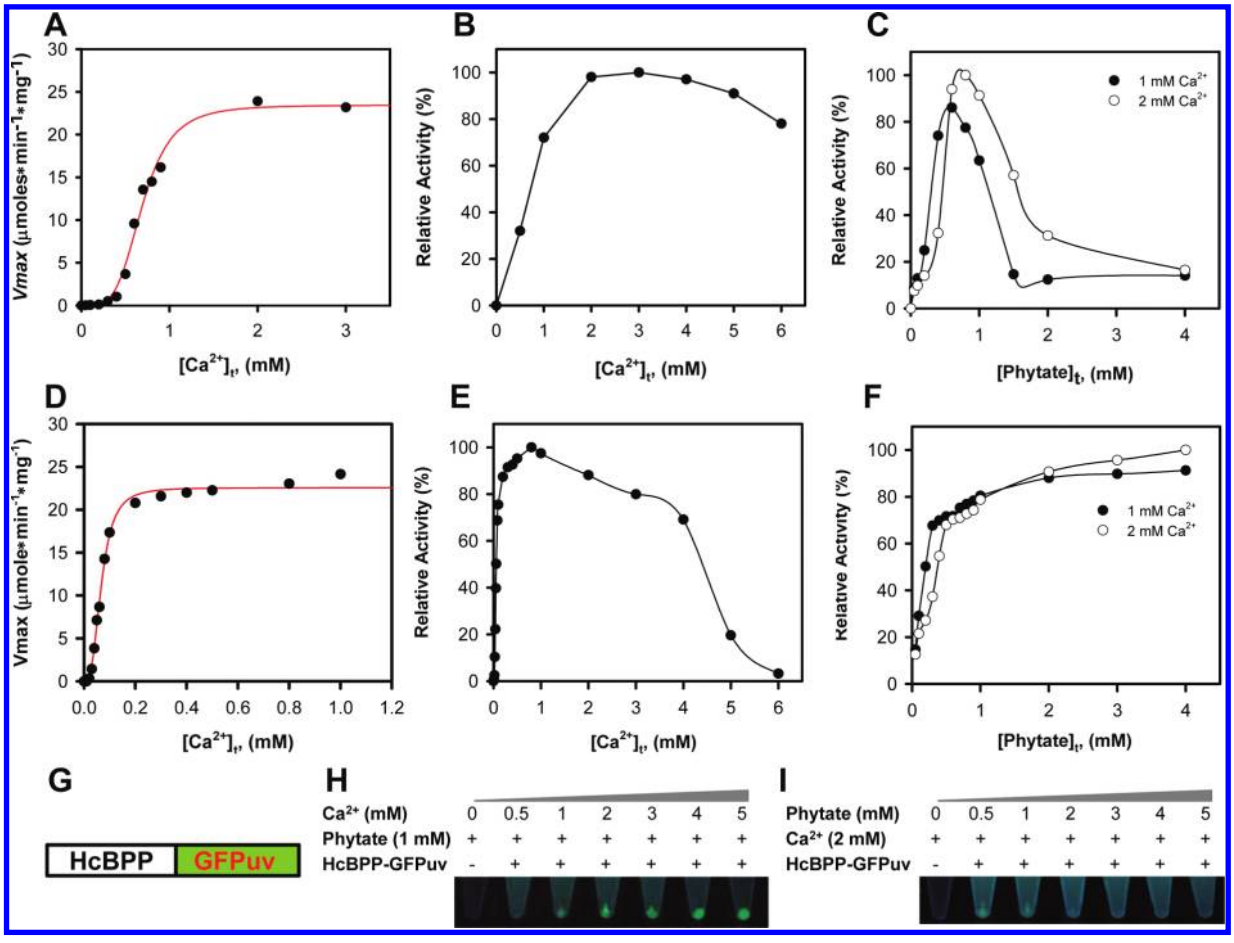

FIGURE 4: Effects of Ca^{2+} and phytate concentrations on β-propeller phytase activity. (A) HcBPP was preincubated with increasing concentrations of Ca^{2+} and then mixed with 1.0 mM phytate preincubated with the same concentration of Ca^{2+} in 50 mM Tris-HCl (pH 7.0). Curves were created by fitting the data generated to the Hill equation. The rate of phytate hydrolysis under each experimental condition is expressed as V (micromoles per minute per milligram). (B) HcBPP activity measured using a single fixed concentration of phytate (1 mM) and Ca^{2+} concentrations ranging from 0 to 6 mM. (C) Phytase activity, measured using a single fixed Ca^{2+} concentration (1 or 2 mM) and phytate concentrations in the range of 0−4.0 mM. (D) BaBPP was preincubated with increasing concentrations of Ca^{2+} and then mixed with 1.0 mM phytate preincubated with the same concentration of Ca^{2+} in 50 mM Tris-HCl (pH 7.0). Curves were created by fitting the data generated to the Hill equation. The rate of phytate hydrolysis under each experimental condition is expressed as V (micromoles per minute per milligram). (E) BaBPP activity measured using a single fixed concentration of phytate (1 mM) and Ca^{2+} concentrations ranging from 0 to 6 mM. (F) Phytase activity measured using a single fixed Ca^{2+} concentration (1 or 2 mM) and phytate concentrations in the range of 0−4.0 mM. (G) Schematic representations of a fusion protein of HcBPP with GFPuv. (H) In vitro visualization showing HcBPP binding to insoluble Ca^{2+}-phytate salts. Recombinants with a fusion protein of HcBPP with GFPuv were incubated with a single fixed phytate concentration of 1 mM and varying concentrations of Ca^{2+} (as indicated) in 50 mM Tris buffer (pH 7.0). (I) In vitro visualization showing HcBPP binding to insoluble Ca^{2+}-phytate salts. Recombinants with a fusion protein of HcBPP with GFPuv were incubated with a single fixed Ca^{2+} concentration of 2 mM and varying phytate concentrations (as indicated) in 50 mM Tris buffer (pH 7.0). In panels H and I, the fusion protein of HcBPP with GFPuv was visualized under ultraviolet light.

We designed a HcBPP−GFPuv fusion protein to address whether the β-propeller phytase can bind insoluble Ca^{2+}-phytate salts visually. After mixing the purified fusion protein (Figure 2B) with the substrate with either a single fixed concentration of phytate with increasing concentrations of Ca^{2+} (Figure 4H) or vice versa (Figure 4I), we centrifuged the mixtures (2 min at 12000 rpm) to visualize how HcBPP bound insoluble Ca^{2+}-phytate salts directly. The results demonstrated that HcBPP specifically binds insoluble Ca^{2+}-phytate salts (Figure 4H), but not Ca^{2+}-free phytate in the reaction mixture (Figure 4I). This supports the unique function and mechanism of the hydrolysis of insoluble Ca^{2+}-phytate salts by β-propeller phytase.

To provide more detailed information about the formation of the Ca^{2+}-phytate complex at a given phytate and Ca^{2+} concentration in the reaction solutions, we calculated [Ca^{2+}], [phytate], [Ca^{2+}-phytate], and [$(Ca^{2+})_3$-phytate] as a function of Ca^{2+} or phytate concentration, based on the measured dissociation constants from the ITC analysis for the Ca^{2+} binding to phytate at pH 5.0. The results shown in panels A and B of Figure 5 clearly indicate that all of the phytate was present as monocalcium-phytate or tricalcium-phytate in the reaction solution containing the lowest total phytate concentration. This is in good agreement with previous findings on the chemical properties of phytate, which can form only insoluble Ca^{2+}-phytate salts when an equivalent or excess amount of Ca^{2+} is added (*45*). In particular, these calculations are consistent with the enzymatic activity profiles of HcBPP, indicating that HcBPP prefers insoluble Ca^{2+}-phytate salt as a substrate with an increasing concentration of Ca^{2+}-phytate (Figure 4B). In contrast, the results shown in panels C and D of Figure 5 indicate that increasing the total phytate concentration at a single fixed concentration significantly increases the amount of Ca^{2+}-free phytate (i.e., not complexed with Ca^{2+}) above an equivalent amount of Ca^{2+} in the reaction mixture. This further explains why the HcBPP activity is

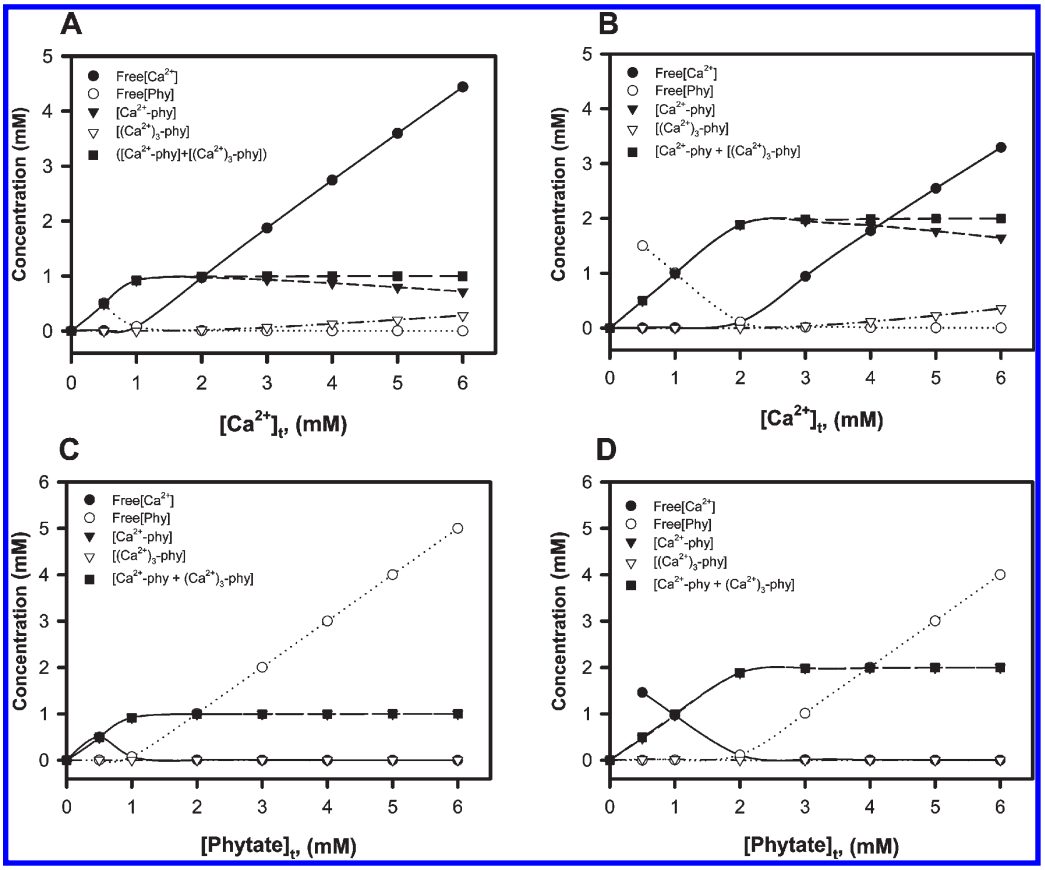

FIGURE 5: Calculated plots of $[Ca^{2+}]$, [phytate], $[Ca^{2+}$-phytate], $[(Ca^{2+})_3$-phytate], and $[Ca^{2+}$-phytate] + $[(Ca^{2+})_3$-phytate] as a function of Ca^{2+} or phytate concentration. Each concentration was calculated from a single fixed phytate concentration of 1 (A) or 2 mM (B) as a function of Ca^{2+} concentration, based on the measured dissociation constants from the ITC analysis of Ca^{2+} binding to phytate at pH 5.0. Each concentration was calculated from a single fixed Ca^{2+} concentration of 1 (C) or 2 mM (D) as a function of phytate concentration, based on the measured dissociation constants from the ITC analysis of Ca^{2+} binding to phytate at pH 5.0.

decreased markedly with an increasing total phytate concentration (Figure 4C), indicating that HcBPP can hydrolyze only insoluble Ca^{2+}-phytate salts. Along with its substrate binding specificity for Ca^{2+}-phytate salts (Figure 4H,I), this strongly suggests that an excess amount of Ca^{2+}-free phytate or free-Ca^{2+}, not complexed with each other, acts as a competitive inhibitor of HcBPP and that insoluble Ca^{2+}-phytate salts is the active or true substrate for HcBPP, not the Ca^{2+}-free phytate.

Identification of the Final Product of HcBPP-Mediated Metabolism of Ca^{2+}-Phytate and Thermodynamics of the Final Product Interactions with Metal Cations. We sought to determine the optimal conditions for the hydrolysis of Ca^{2+}-phytate by HcBPP. As shown in Figure 4, a molar ratio of Ca^{2+} to phytate of 3:1 was optimal for the enzymatic activity of HcBPP. We thus performed a time course analysis of the total amounts of phosphate liberated from tricalcium-phytate salts, prepared by mixing 1 mM Na-phytate and 3 mM Ca^{2+} at 55 °C in Tris-HCl at pH 7.0. Aliquots from each reaction mixture were periodically removed, and the total amounts of liberated phosphate were quantified. The concentration of phosphate liberated as a result of the hydrolysis of Ca^{2+}-phytate salts was very close to 3 mM, indicating that HcBPP hydrolyzed three phosphate groups per phytate molecule (Figure 6A). This result is similar for BaBPP (*17*) in terms of the hydrolytic pattern and the number of phosphate groups hydrolyzed. However, HcBPP hydrolyzed insoluble Ca^{2+}-phytate salts more efficiently than BaBPP did, which prefers monocalcium-phytate salts.

To identify the final products of Ca^{2+}-phytate hydrolysis catalyzed by HcBPP, we further analyzed the reaction products by HPIC. The hydrolysis by HcBPP yielded Ins(2,4,6)P_3 and three phosphate groups as final products (Figure 6B). Ins(2,4,6)P_3 is also the final product of hydrolysis catalyzed by BaBPP (*17*). HPIC analysis further identified Ins(2,4,5,6)P_4 as a reaction intermediate (Figure 6B). On the basis of our kinetic data and the results of HPIC analysis of reaction intermediates and final products, we propose the existence of a sequential hydrolytic pathway (Figure 6C). HcBPP preferentially recognizes insoluble Ca^{2+}-phytate salts and initially hydrolyzes Ca^{2+}-phytate at the D-3 position. The enzyme subsequently binds to the bidentate ligand Ins(1,2,4,5,6)P_5 and sequentially hydrolyzes the D-1 phosphate group, releasing Ins(2,4,5,6)P_4, and finally the D-5 phosphate group, yielding Ins(2,4,6)P_3 as the final product (Figure 6C).

To examine the chelation properties of Ins(2,4,6)P3, the final product of the hydrolytic reaction catalyzed by HcBPP, we purified Ins(2,4,6)P_3 by HPLC and analyzed the thermodynamic parameters of its binding to metal cations by ITC. The results indicated that Ins(2,4,6)P_3 is unable to bind Ca^{2+} or any other cation tested, including Co^{2+}, Cu^{2+}, Fe^{3+}, Mg^{2+}, Mn^{2+}, Sr^{2+}, and Zn^{2+} (Figure 7). We believe that the absence of adjacent phosphate groups in Ins(2,4,6)P_3 prevents the formation of bidentate complexes with metal cations. In addition, the long distances (6.7 Å) between the phosphate groups of Ins(2,4,6)P_3 may be too large to form complexes with cations. Thus, HcBPP efficiently eliminates phytate's chelation of not only Ca^{2+} but also other important metal cations and in so doing provides metal cations and phosphate groups as nutrients for ocean-dwelling bacteria such as *H. chejuensis*.

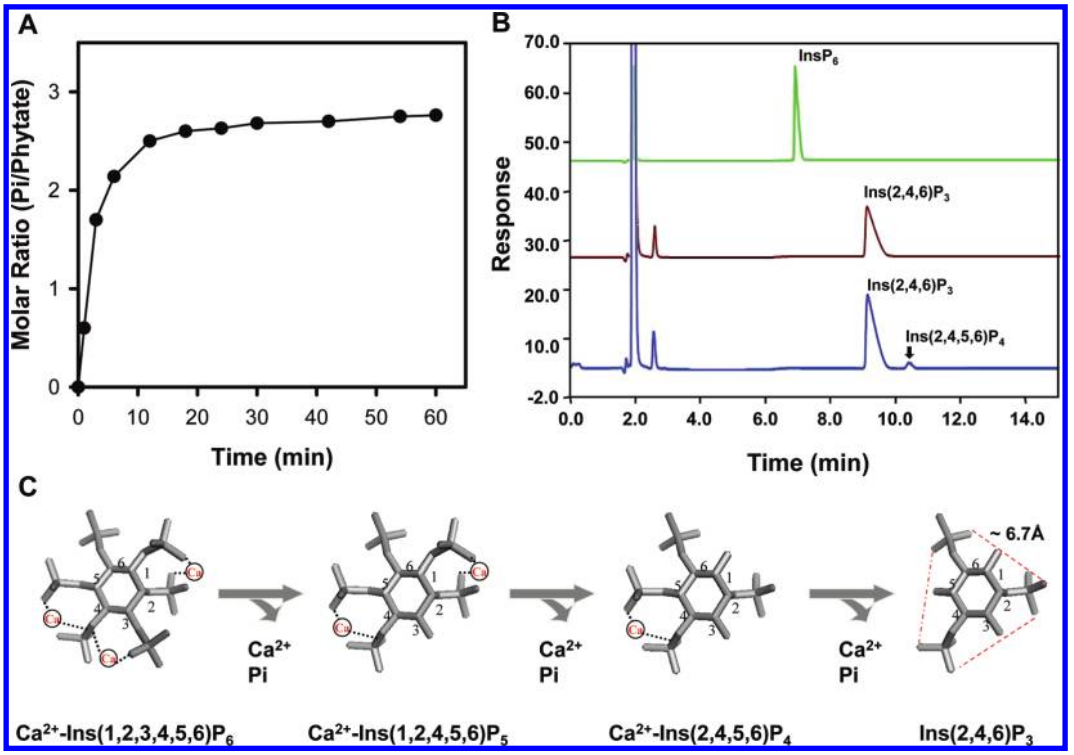

FIGURE 6: Time course analysis of the liberation of phosphate from Ca^{2+}-phytate by HcBPP, HPIC analysis of the reaction products, and schematic representation of the proposed hydrolytic pathway. (A) Time course analysis of the hydrolysis of Ca^{2+}-phytate using a substrate prepared by mixing 1 mM Ca^{2+} and 1 mM phytate. The concentration of phosphate liberated as a result of the hydrolysis of Ca^{2+}-phytate was very close to 3 mM, indicating that HcBPP hydrolyzed three phosphate groups per phytate molecule. (B) To determine their identities, we analyzed the final reaction products of the hydrolysis of Ca^{2+}-phytate by HcBPP by HPIC. (C) The reference spectrum shows the products of BaBPP-mediated hydrolysis.

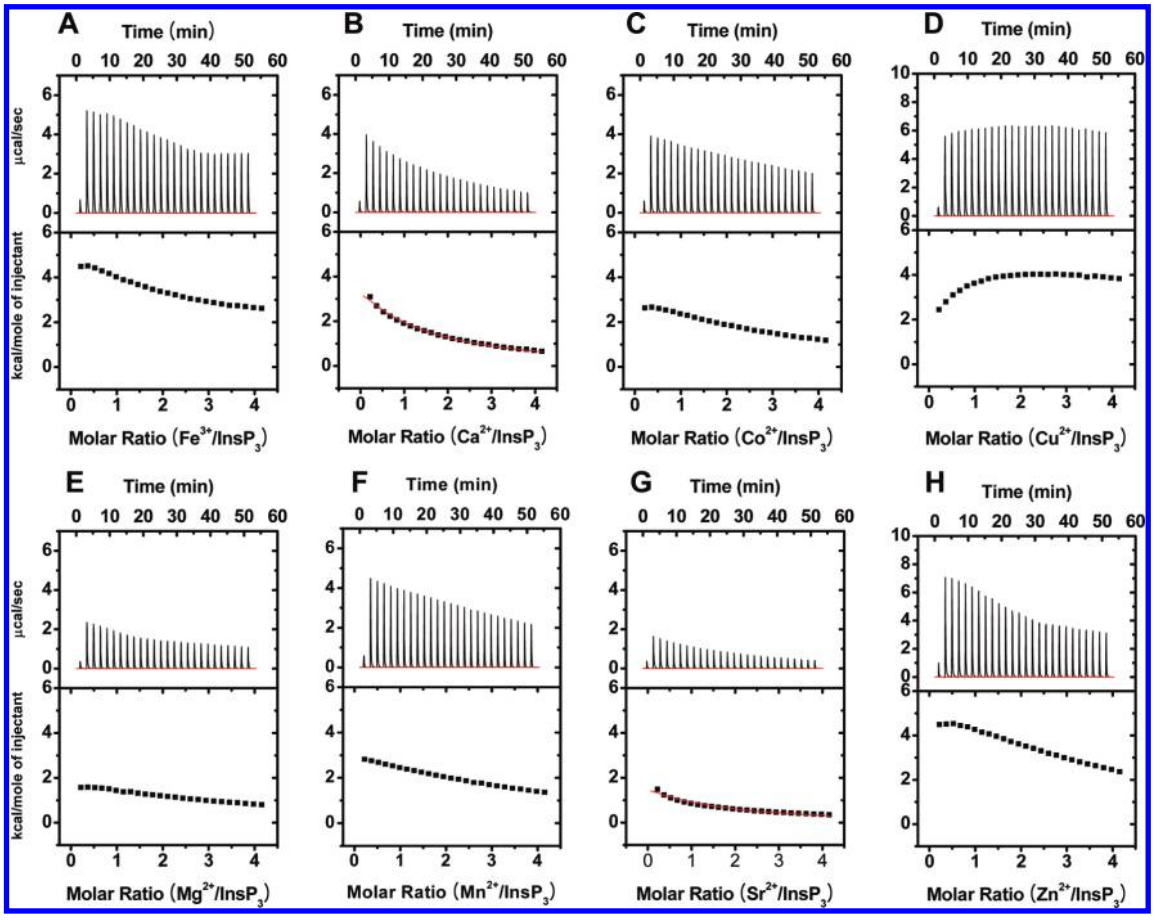

FIGURE 7: ITC analysis of the binding of various metal ions to Ins(2,4,6)P_3. ITC was used to study the kinetics of binding of Fe^{2+}, Ca^{2+}, Cu^{2+}, Co^{2+}, Mg^{2+}, Mn^{2+}, Sr^{2+}, and Zn^{2+} ions to Ins(2,4,6)P_3 at pH 5.0 and 37 °C. For each titration, raw data are shown in the top panel and integrated heat data (corrected for dilution) are shown in the bottom panel.

DISCUSSION

The antinutritional impact of phytate has been documented in numerous papers and reviews detailing its physicochemical properties and various biological functions. Phytate chelates nutritionally important minerals, including calcium, magnesium, copper, iron, zinc, cobalt, and manganese ions (*1*−*3*, *46*). The resulting complexes are insoluble, difficult for the human GI tract to hydrolyze during digestion, and thus typically not absorbed (*2*, *3*, *39*). Nonetheless, few reports have presented quantitative data related to its interactions with divalent and trivalent cations, not only because of phytate's relatively sophisticated chemical structure but also as a result of its tremendous ability to chelate various divalent and trivalent cations, including Ca^{2+}, Co^{2+}, Cu^{2+}, Fe^{3+}, Mg^{2+}, Mn^{2+}, Sr^{2+}, and Zn^{2+} (*17*). To obtain information about the function of phytate in natural aqueous solutions, we have successfully applied well-established ITC techniques to generate quantitative data describing the interaction of phytate with these cations. ITC is a valuable experimental tool that facilitates quantification of the thermodynamic parameters that characterize binding processes, by virtue of its ease of application and high level of precision. Ultimately, this approach provided us with thermodynamic data that allowed us to confirm the binding model, quantify the binding enthalpy (ΔH) and entropy ($T\Delta S$), and determine the binding constants (K_a).

The results of our ITC analysis showed that phytate binds divalent and trivalent ions with high affinity (K_d = 0.77−151 μM). The strong binding affinity of phytate for Fe^{3+} corroborates the results of previous studies (*47*, *48*). The order of the relative stoichiometries of the complexes formed between metal cations and phytate was as follows: $Ca^{2+} > Cu^{2+} > Mn^{2+} > Zn^{2+} > Mg^{2+} > Co^{2+} > Sr^{2+}$. The order of the relative stabilities of the phytate-mineral salts that formed, calculated from thermodynamic parameters, was as follows: $Zn^{2+} > Fe^{3+} > Ca^{2+} > Mn^{2+} > Cu^{2+} > Co^{2+} > Mg^{2+} > Sr^{2+}$. Thus, it is possible that Zn^{2+} forms the most stable cation-phytate salts, once bound. Our results indicate that phytate forms insoluble mono- and disubstituted salts with most of the tested metal cations, with the exception of Ca^{2+}, with which it formed insoluble tetracalcium-phytate salts (Figure 1 and Table 1). Studies on the effects of pH on interactions between Ca^{2+} and phytate over a wide pH range (2.0−9.0) confirmed the uniqueness of the binding interaction between Ca^{2+} and phytate. Calcium and phytate primarily form stable, insoluble tricalcium- or tetracalcium-phytate salts in the pH range of 3.0−9.0. At lower pH values, it forms monocalcium-phytate salts (Figure 2 and Table 2). These results are supported by previous studies, which showed that the low pH in gastric environments fosters the formation of calcium-phytate salts in the stomach following the ingestion of soy protein isolate (*49*). These mineral-phytate salts are considered a key cause of the reduced Ca^{2+} bioavailability of diets high in phytate, because monogastric animals such as poultry, pigs, and humans secrete insufficient amounts of intestinal phytase to degrade them (*3*, *8*, *9*, *39*).

Undigested mineral-phytate salts in monogastric animals are eliminated as waste and may be a major source of phytate in aquatic systems (*50*). Phytate has been detected in rivers and oceans, as well as in lake and marine sediments (*51*). It rapidly forms complexes with Ca^{2+} when introduced into marine environments, possibly because of the high levels of dissolved Ca^{2+}. Insoluble Ca^{2+}-phytate salts ultimately sink from the surface of the ocean, although they can be hydrolyzed by β-propeller phytases produced by ocean-dwelling bacteria such as *S. oneidensis* (*18*) and *P. nyacknesis* (*20*, *52*). A lack of useful experimental data has limited our understanding of how β-propeller phytases hydrolyze insoluble Ca^{2+}-phytate salts in the sea.

We cloned a novel β-propeller phytase from the marine bacterium *H. chejuensis*, which preferentially hydrolyzes insoluble Ca^{2+}-phytate salts. Structure-based sequence alignments indicated that HcBPP may have evolutionarily acquired multiple calcium-binding sites in its active site cleft, which contains a significant number of negatively charged side chains (provided by the long loops that separate the β-sheets) and thus provides a favorable electrostatic environment for the binding of insoluble tricalcium- or tetracalcium-phytate salts (Figure S1 of the Supporting Information and Figure 4H). This is consistent with our ITC data on the binding of Ca^{2+} by phytate, which indicated that three or four molecules of Ca^{2+} bind with high affinity to each phytate molecule [in the pH range of 3.0−9.0 (Figure 2 and Table 2)]. Further biochemical and kinetic analyses confirmed that HcBPP required a high concentration of Ca^{2+} to hydrolyze phytate. Its activity peaked when the molar ratio of Ca^{2+} to phytate was approximately 3−4, a ratio that favors the formation of insoluble Ca^{2+}-phytate salts (Figure 4B). Finally, we showed that HcBPP catalyzed the removal of up to three phosphate groups from insoluble Ca^{2+}-phytate salts (Figure 6A). The final product was identified as Ins(2,4,6)P_3, indicating that the enzyme preferentially binds bidentate (P-Ca^{2+}-P) Ca^{2+}-phytate salts and that it hydrolyzes every second phosphate, ultimately yielding three phosphate ions per molecule of Ins(2,4,6)P_3 (Figure 6B,C). ITC analysis of Ins(2,4,6)P_3 in combination with several metal cations further demonstrated that HcBPP abrogated phytate's potent ability to chelate several metal cations, and that it released free phosphate and Ca^{2+} ions from insoluble Ca^{2+}-phytate salts that may serve as nutrients for marine bacteria (Figure 7).

On the basis of various experimental approaches in this article and our previous papers (*15*−*17*), we have several lines of evidence that show that β-propeller phytase hydrolyzes insoluble Ca^{2+}-phytate salts. First, the chemical properties of phytate have shown that the phytate can form insoluble Ca^{2+}-phytate salts only when an equivalent or excess amount of Ca^{2+} is added. Under such conditions, the filtrates are clear and contain only a trace of Ca^{2+}-free phytate (*45*). This was further demonstrated by the calculation of the fractions of Ca^{2+}-phytate and phytate, based on the measured dissociation constants from the ITC analysis of Ca^{2+} binding to a phytate solution. Those results indicated that all of the phytate was present as Ca^{2+}-phytate or $(Ca^{2+})_3$-phytate when an equivalent or excess amount of Ca^{2+} was added to the reaction solution (Figure 5A,B). Thus, we believe that the β-propeller phytases are able to hydrolyze insoluble Ca^{2+}-phytate salts, instead of trace amounts of soluble phytate in the reaction mixtures. Second, when all of the phytate is present as insoluble Ca^{2+}-phytate salts, the β-propeller phytase can sequentially hydrolyze one of the phosphate groups in the bidentate (P-Ca^{2+}-P) form of the insoluble Ca^{2+}-phytate salts to yield a myo-inositol 2,4,6-trisphosphate and three phosphates as final products. Thus, if it hydrolyzes a trace amount of soluble phytate at a high Ca^{2+} concentration, when most phytate is present as Ca^{2+}-phytate salts, the β-propeller phytase would not completely hydrolyze 3 mol of phosphate groups per phytate.

The molecular mechanism of the β-propeller phytases for the hydrolysis of insoluble Ca^{2+}-phytate salts may result from its substrate binding specificity for the Ca^{2+}-bidentate (P-Ca^{2+}-P) form of the insoluble Ca^{2+}-phytate salts at the active site of the

enzyme (*17*) (Figure 4H,I). Moreover, the β-propeller phytases are incapable of hydrolyzing myo-inositol 2,4,6-trisphosphate, because of a lack of Ca^{2+} binding properties and the long distance between the two phosphate groups of myo-inositol 2,4,6-trisphosphate (Figures 6C and 7). Finally, the crystal structure of BaBPP in the two-phosphate-bound state provided direct evidence that β-propeller phytase selectively binds insoluble Ca^{2+}-phytate salts as a substrate (*15*, *17*). The molecular mechanism for the insoluble Ca^{2+}-phytate salts may result from the specific active site environment, composed primarily of negatively charged amino acid residues for the favorable binding of insoluble Ca^{2+}-phytate salts (*15*).

Under physiological conditions, it is likely that phytate exists in the form of complexes with biologically important trivalent and divalent cations such as Fe^{3+}, Ca^{2+}, Mg^{2+}, and Zn^{2+}, as has been shown in plant seeds (*1*, *2*). Of the complexes formed, Ca^{2+}-phytate salts may be more prevalent, because Ca^{2+} is the most abundant divalent cation in processed human food and animal feed (*1*, *3*, *46*), and because ITC analysis indicated that phytate has multiple calcium binding sites (Figure 2 and Table 2). The insolubility of these salts is considered the major reason for the reduced bioavailability of divalent cations in foods with a high phytate content. We have identified some of the kinetic mechanisms that explain how β-propeller phytases metabolize these insoluble mineral-phytate salts, and the biotechnological applications that may be developed to weaken the antinutritional effects of phytate, especially in cereal-based foods with high phytate contents.

In conclusion, we demonstrated that HcBPP efficiently hydrolyzes insoluble Ca^{2+}-phytate salts and completely abrogates the ability of phytate to chelate certain metal ions. Our data indicate that BPP enzymes may be useful for weakening the antinutritional effects of phytate on minerals that are biologically important to humans.

ACKNOWLEDGMENT

We thank Dr. J.-F. Kim for generously providing *H. chejuensis* KCTC 2396 chromosomal DNA and P.-S. Oh for helpful discussions.

SUPPORTING INFORMATION AVAILABLE

Structure-based sequence alignment of HcBPP with BPPs from *Bacillus* species (Figure S1) and SDS−PAGE of purified HcBPP and HcBPP−GFPuv fusion protein (Figure S2). This material is available free of charge via the Internet at http://pubs.acs.org.

NOTE ADDED AFTER ASAP PUBLICATION

After this paper was published ASAP October 21, 2010, corrections were made to Figure 1A and the captions of Figures 1 and 4. The revised version was published November 3, 2010.

REFERENCES

1. Reddy, N. R., Sathe, S. K., and Salunkhe, D. K. (1982) Phytates in legumes and cereals. *Adv. Food Res. 28*, 1–92.
2. Reddy, N. R., and Sathe, S. H. (2002) Food phytates, pp 1−223, CRC Press, Boca Raton, FL.
3. Raboy, V. (2001) Seeds for a better future: 'Low phytate' grains help to overcome malnutrition and reduce pollution. *Trends Plant Sci. 6*, 458–462.
4. Torre, M., Rodriguez, A. R., and Saura-Calixto, F. (1991) Effects of dietary fiber and phytic acid on mineral availability. *Crit. Rev. Food Sci. Nutr. 30*, 1–22.
5. Bruce, H. M., and Callow, R. K. (1934) Cereals and rickets. The role of inositol hexaphosphoric acid. *Biochem. J. 28*, 517–528.
6. Harrison, D. C., and Mellanby, E. (1939) Phytic acid and the rickets-producing action of cereals. *Biochem. J. 33*, 1660–1680.
7. Mellanby, E. (1949) The rickets-producing and anti-calcifying action of phytate. *J. Physiol. 109*, 488–533.
8. McCance, R. A., and Widdowson, E. M. (1942) Mineral metabolism on dephytinized bread. *J. Physiol. 101*, 304–313.
9. McCance, R. A., and Widdowson, E. M. (1942) Mineral metabolism of healthy adults on white and brown bread dietaries. *J. Physiol. 101*, 44–85.
10. Mullaney, E. J., and Ullah, A. H. (2003) The term phytase comprises several different classes of enzymes. *Biochem. Biophys. Res. Commun. 312*, 179–184.
11. Oh, B. C., Choi, W. C., Park, S., Kim, Y. O., and Oh, T. K. (2004) Biochemical properties and substrate specificities of alkaline and histidine acid phytases. *Appl. Microbiol. Biotechnol. 63*, 362–372.
12. Kerovuo, J., Lauraeus, M., Nurminen, P., Kalkkinen, N., and Apajalahti, J. (1998) Isolation, characterization, molecular gene cloning, and sequencing of a novel phytase from *Bacillus subtilis*. *Appl. Environ. Microbiol. 64*, 2079–2085.
13. Kim, Y. O., Lee, J. K., Kim, H. K., Yu, J. H., and Oh, T. K. (1998) Cloning of the thermostable phytase gene (phy) from *Bacillus* sp. DS11 and its overexpression in *Escherichia coli*. *FEMS Microbiol. Lett. 162*, 185–191.
14. Ha, N. C., Oh, B. C., Shin, S., Kim, H. J., Oh, T. K., Kim, Y. O., Choi, K. Y., and Oh, B. H. (2000) Crystal structures of a novel, thermostable phytase in partially and fully calcium-loaded states. *Nat. Struct. Biol. 7*, 147–153.
15. Shin, S., Ha, N. C., Oh, B. C., Oh, T. K., and Oh, B. H. (2001) Enzyme mechanism and catalytic property of β propeller phytase. *Structure 9*, 851–858.
16. Oh, B. C., Chang, B. S., Park, K. H., Ha, N. C., Kim, H. K., Oh, B. H., and Oh, T. K. (2001) Calcium-dependent catalytic activity of a novel phytase from *Bacillus amyloliquefaciens* DS11. *Biochemistry 40*, 9669–9676.
17. Oh, B. C., Kim, M. H., Yun, B. S., Choi, W. C., Park, S. C., Bae, S. C., and Oh, T. K. (2006) Ca^{2+}-inositol phosphate chelation mediates the substrate specificity of β-propeller phytase. *Biochemistry 45*, 9531–9539.
18. Cheng, C., and Lim, B. L. (2006) β-Propeller phytases in the aquatic environment. *Arch. Microbiol. 185*, 1–13.
19. Lim, B. L., Yeung, P., Cheng, C., and Hill, J. E. (2007) Distribution and diversity of phytate-mineralizing bacteria. *ISME J. 1*, 321–330.
20. Huang, H., Shao, N., Wang, Y., Luo, H., Yang, P., Zhou, Z., Zhan, Z., and Yao, B. (2009) A novel β-propeller phytase from *Pedobacter nyackensis* MJ11 CGMCC 2503 with potential as an aquatic feed additive. *Appl. Microbiol. Biotechnol. 83*, 249–259.
21. MicroCal (2002) ITC data analysis in Origin: Tutorial guide, using Origin scientific plotting software to analyze calorimetric data from all MicroCal isothermal titration calorimeters, pp 100-106, MicroCal, Northampton, MA.
22. Plackett, R. L. (1983) Karl Pearson and the Chi-squared test. *Int. Stat. Rev. 51*, 59–72.
23. Wiseman, T., Williston, S., Brandts, J. F., and Lin, L. N. (1989) Rapid measurement of binding constants and heats of binding using a new titration calorimeter. *Anal. Biochem. 179*, 131–137.
24. Talamond, P., Doulbeau, S., Rochette, I., and Guyot, J. P. (2000) Anion-exchange high-performance liquid chromatography with conductivity detection for the analysis of phytic acid in food. *J. Chromatogr., A 871*, 7–12.
25. Cheryan, M. (1980) Phytic acid interactions in food systems. *Crit. Rev. Food Sci. Nutr. 13*, 297–335.
26. Sandstead, H. H. (1992) Fiber, phytates, and mineral nutrition. *Nutr. Rev. 50*, 30–31.
27. Harland, B. F. (1989) Dietary fiber and mineral bioavailability. *Nutr. Res. Rev. 2*, 133–147.
28. Harland, B. F., and Oberleas, D. (1987) Phytate in foods. *World Rev. Nutr. Diet. 52*, 235–259.
29. Harinarayan, C. V., Ramalakshmi, T., and Venkataprasad, U. (2004) High prevalence of low dietary calcium and low vitamin D status in healthy south Indians. *Asia Pac. J. Clin. Nutr. 13*, 359–364.
30. Harinarayan, C. V., Ramalakshmi, T., Prasad, U. V., Sudhakar, D., Srinivasarao, P. V., Sarma, K. V., and Kumar, E. G. (2007) High prevalence of low dietary calcium, high phytate consumption, and vitamin D deficiency in healthy south Indians. *Am. J. Clin. Nutr. 85*, 1062–1067.
31. Harinarayan, C. V. (2005) Prevalence of vitamin D insufficiency in postmenopausal south Indian women. *Osteoporosis Int. 16*, 397–402.
32. Brune, M., Rossander, L., and Hallberg, L. (1989) Iron absorption: No intestinal adaptation to a high-phytate diet. *Am. J. Clin. Nutr. 49*, 542–545.
33. Brune, M., Rossander-Hulten, L., Hallberg, L., Gleerup, A., and Sandberg, A. S. (1992) Iron absorption from bread in humans: Inhibiting effects of cereal fiber, phytate and inositol phosphates with different numbers of phosphate groups. *J. Nutr. 122*, 442–449.

34. Hallberg, L., Brune, M., and Rossander, L. (1989) Iron absorption in man: Ascorbic acid and dose-dependent inhibition by phytate. *Am. J. Clin. Nutr. 49*, 140–144.
35. Hallberg, L., Rossander, L., and Skanberg, A. B. (1987) Phytates and the inhibitory effect of bran on iron absorption in man. *Am. J. Clin. Nutr. 45*, 988–996.
36. Sandberg, A. S., Brune, M., Carlsson, N. G., Hallberg, L., Skoglund, E., and Rossander-Hulthen, L. (1999) Inositol phosphates with different numbers of phosphate groups influence iron absorption in humans. *Am. J. Clin. Nutr. 70*, 240–246.
37. Gibson, R. S. (1994) Content and bioavailability of trace elements in vegetarian diets. *Am. J. Clin. Nutr. 59*, 1223S–1232S.
38. Gibson, R. S., Donovan, U. M., and Heath, A. L. (1997) Dietary strategies to improve the iron and zinc nutriture of young women following a vegetarian diet. *Plant Foods Hum. Nutr.* (*Dordrecht, Neth.*) *51*, 1–16.
39. Raboy, V., and Dickinson, D. B. (1984) Effect of Phosphorus and Zinc Nutrition on Soybean Seed Phytic Acid and Zinc. *Plant Physiol. 75*, 1094–1098.
40. Grynspan, F., and Cheryan, M. (1983) Calcium phytate: Effect of pH and molar ratio on in vitro solubility. *J. Am. Oil Chem. Soc. 60*, 1761–1764.
41. Marini, M. A., Evans, W. J., and Morris, N. M. (1985) Calorimetric and potentiometric studies on the binding of calcium by phytic acid. *J. Appl. Biochem. 7*, 180–191.
42. Chan, W. L., Lung, S. C., and Lim, B. L. (2006) Properties of β-propeller phytase expressed in transgenic tobacco. *Protein Expression Purif. 46*, 100–106.
43. Kerovuo, J., Lappalainen, I., and Reinikainen, T. (2000) The metal dependence of *Bacillus subtilis* phytase. *Biochem. Biophys. Res. Commun. 268*, 365–369.
44. Tye, A. J., Siu, F. K., Leung, T. Y., and Lim, B. L. (2002) Molecular cloning and the biochemical characterization of two novel phytases from *B. subtilis* 168 and *B. licheniformis*. *Appl. Microbiol. Biotechnol. 59*, 190–197.
45. Yang, E. F. (1940) Ionization of Calcium Phytate. *Nature 145*, 745.
46. Raboy, V. (2007) The ABCs of low-phytate crops. *Nat. Biotechnol. 25*, 874–875.
47. Sandberg, A. S. (2002) Bioavailability of minerals in legumes. *Br. J. Nutr. 88* (Suppl. 3), S281–S285.
48. Morris, E. R., and Ellis, R. (1980) Bioavailability to rats of iron and zinc in wheat bran: Response to low-phytate bran and effect of the phytate/zinc molar ratio. *J. Nutr. 110*, 2000–2010.
49. Champagne, E. T. (1988) Effects of pH on mineral-phytate, protein-mineral-phytate, and mineral-fiber interactions. Possible consequences of atrophic gastritis on mineral bioavailability from high-fiber foods. *J. Am. Coll. Nutr. 7*, 499–508.
50. Suzumura, M., and Kamatani, A. (1995) Origin and distribution of inositol hexaphosphate in estuarine and coastal sediments. *Limnol. Oceanogr. 40*, 1254–1261.
51. Suzumura, M., and Kamatani, A. (1993) Isolation and determination of inositol hexaphosphate in sediments from Tokyo Bay. *Geochim. Cosmochim. Acta 57*, 2197–2202.
52. Huang, H., Shi, P., Wang, Y., Luo, H., Shao, N., Wang, G., Yang, P., and Yao, B. (2009) Diversity of β-propeller phytase genes in the intestinal contents of grass carp provides insight into the release of major phosphorus from phytate in nature. *Appl. Environ. Microbiol. 75*, 1508–1516.